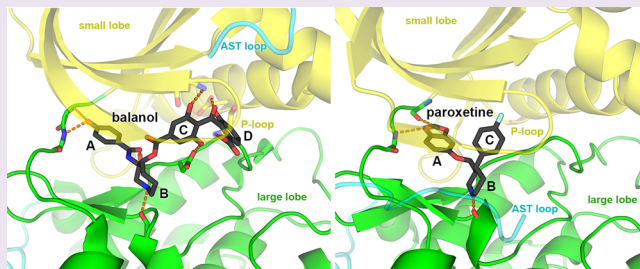


# Molecular Basis for Small Molecule Inhibition of G Protein-Coupled Receptor Kinases

Kristoff T. Homan and John J. G. Tesmer\*

Life Sciences Institute, Departments of Pharmacology and Biological Chemistry, University of Michigan, Ann Arbor, Michigan 48109, United States

**ABSTRACT:** Small molecules that inhibit the protein kinase A, G, and C (AGC) family of serine/threonine kinases can exert profound effects on cell homeostasis and thereby regulate fundamental processes such as heart rate, blood pressure, and metabolism, but there is not yet a clinically approved drug in the United States selective for a member of this family. One subfamily of AGC kinases, the G protein-coupled receptor (GPCR) kinases (GRKs), initiates the desensitization of active GPCRs. Of these, GRK2 has been directly implicated in the progression of heart failure. Thus, there is great interest in the identification of GRK2-specific chemical probes that can be further developed into therapeutics. Herein, we compare crystal structures of small molecule inhibitors in complex with GRK2 to those of highly selective compounds in complex with Rho-associated coiled-coil containing kinase 1 (ROCK1), a closely related AGC kinase. This analysis suggests that reduced hydrogen-bond formation with the hinge of the kinase domain, occupation of the hydrophobic subsite, and, consequently, higher buried surface area are key drivers of potency and selectivity among GRK inhibitors.



Over the past several decades, many potent, selective small molecule drugs targeting G protein-coupled receptors (GPCRs) have been generated and now serve as front-line therapeutic interventions in treating human diseases ranging from schizophrenia/bipolar disorder<sup>1</sup> to asthma.<sup>2</sup> Along with a dramatic recent increase in our structural understanding of GPCRs,<sup>3–5</sup> there has been a parallel increase in efforts to achieve “softer control” of GPCR signaling via allosteric modulators,<sup>6</sup> molecules capable of biased signaling,<sup>7</sup> and compounds that inhibit GTPase activating proteins acting on heterotrimeric G proteins.<sup>8</sup> Another soft approach to modulate GPCR signaling is to inhibit GPCR kinases (GRKs), a subfamily of the protein kinase A (PKA), G, and C (AGC) branch of the kinase<sup>9</sup> that initiates the desensitization of activated GPCRs through phosphorylation of Ser/Thr residues in the third intracellular loop and/or carboxyl terminal tail of the receptor.<sup>10</sup> These covalent modifications promote the binding of arrestins, which not only uncouple the receptors from heterotrimeric G proteins and target them for endocytosis but also instigate G protein-independent signaling pathways.<sup>11,12</sup> Thus, inhibiting GRKs, which would block arrestin-dependent processes, can enhance G protein-dependent signaling through GPCRs. Consequently, coadministration of a specific GRK inhibitor may allow use of lower doses of drugs that serve as agonists at GPCRs, thereby alleviating off-target effects. In support of this idea, Raf kinase inhibitor protein inhibits GRK2 in the heart, thereby enhancing signaling through  $\beta$  adrenergic receptors and contractility responses,<sup>13</sup> and GRK5-deficient mice exhibit enhanced muscarinic sensitivity.<sup>14</sup>

Individual GRKs are also relevant drug targets in their own right.<sup>15–17</sup> Phosphorylation of dopamine D<sub>1</sub> receptors in the kidney by activating mutations in GRK4 is believed to cause essential hypertension,<sup>18</sup> and inhibition of GRK5 is reported to protect against cardiac hypertrophy.<sup>19</sup> However, among these enzymes, the most well-established drug target, and the chief focus of this review, is GRK2, an enzyme strongly implicated in the progression of heart failure. In this pathophysiological state, a 3-fold increase of GRK2 protein and mRNA levels is observed<sup>20–22</sup> and thought to underlie downregulation of  $\beta_1$ -adrenergic receptors, resulting in reduced cAMP levels and contractility. Mouse models that overexpress GRK2 in the heart recapitulate much of this phenotype.<sup>23,24</sup> Studies using a cardiac-specific GRK2 gene deletion or a cardiac-specific expression of a dominant negative protein domain derived from the C-terminal portion of GRK2 (GRK2ct, also known as  $\beta$ ARKct) showed that reduction of GRK2 activity improves outcomes in mouse models of heart failure.<sup>25–28</sup> When myocytes are transfected with GRK2ct, free G $\beta\gamma$  subunits are sequestered and translocation of GRK2 to the membrane is attenuated, leading to significantly increased cAMP accumulation in cells stimulated with isoproterenol.<sup>29</sup> Furthermore, overexpression of GRK2ct in a murine model of heart failure completely reversed heightened  $\beta$ AR desensitization, as measured by responsiveness to isoproterenol *in vivo* and

**Special Issue:** New Frontiers in Kinases

**Received:** May 20, 2014

**Accepted:** June 25, 2014

**Published:** July 1, 2014

isoproterenol-stimulated membrane adenylyl cyclase activity *in vitro*, and prevented development of cardiomyopathy.<sup>30</sup> More recently in a preclinical porcine model, heart failure was ameliorated by viral-mediated GRK2ct administration.<sup>31</sup> The beneficial impacts of GRK2 inhibition are not limited to the myocardium, as GRK2ct delivered to the adrenal gland resulted in lower sympathetic tone and improved cardiac  $\beta$ AR signaling and function.<sup>32</sup> Thus, it is likely that systemic inhibition of GRK2 would be of therapeutic benefit during heart failure.

However, clinically useful small molecule inhibitors of GRK2 and other GRKs have yet to be described. This review highlights recent developments in the identification and structural analysis of small molecule GRK inhibitors. We begin by discussing what is known about small molecules that target other AGC kinase subfamilies, seeking to identify molecular clues that could lead to the rational design of more potent GRK inhibitors and avoidance of off-target effects.

## ■ AGC KINASE DOMAIN STRUCTURE

In response to the activation of cell surface receptors and other physiological cues, AGC kinases phosphorylate serine and/or threonine residues on various intracellular targets involved in cell homeostasis. AGC kinases are understood very well at the structural level thanks to seminal work by the Taylor lab on cAMP-dependent protein kinase (PKA).<sup>33–35</sup> Although many AGC kinases contain additional regulatory domains or subunits, their catalytic cores are highly conserved and consist of three elements (Figure 1a). The first two are homologous to those found in all protein kinases: a small (or N) lobe composed of an antiparallel  $\beta$ -sheet along with a few  $\alpha$  helices and a large (or C) lobe composed primarily of  $\alpha$ -helices that forms the primary binding site for protein substrates. The active site is formed at the interface of these two domains and is the binding site for most known AGC kinase small molecule inhibitors. In many AGC kinase domains, interaction with  $2\text{Mg}^{2+}\cdot\text{ATP}$  drives closure of the active site cleft such that catalytic residues and the bound polypeptide substrate on the large lobe are brought into close proximity with the  $\gamma$ -phosphate of ATP. This closed conformation, typified by the structure of PKA conducting phosphotransfer on the ATP analogue adenosine 5'-( $\beta,\gamma$ -imido)triphosphate (AMPPNP),<sup>33</sup> is believed to represent the catalytically active configuration of all AGC kinases (Figure 1a). On the basis of the interactions of ATP in this state, three distinct subsites have been defined for small molecule inhibitors that bind in the active site: the adenine, ribose, and polyphosphate subsites.<sup>36</sup> Some inhibitors also take advantage of a fourth pocket adjacent to the polyphosphate subsite known as the hydrophobic subsite (Figure 1b). Small molecules that bind in the active site cleft typically induce a change in the relative positions of the small and large lobes, in part because the hinge that mediates domain closure typically forms direct interactions with compounds that occupy the adenine subsite and also because the two lobes can often adjust their relative orientation to optimize contacts with the bound inhibitor.

The third element of the AGC catalytic core, found in all members except phosphoinositide-3-phosphate dependent protein kinase 1 (PDK1), is a C-terminal extension (C-tail) that interacts both lobes of the kinase domain and contributes to the active site when the kinase domain is in a closed conformation. Three regions of the C-tail have been defined: the C-lobe tether, which forms extensive interactions with the large lobe of the kinase domain, the active site tether (AST), which typically contributes residues into the active site, and the

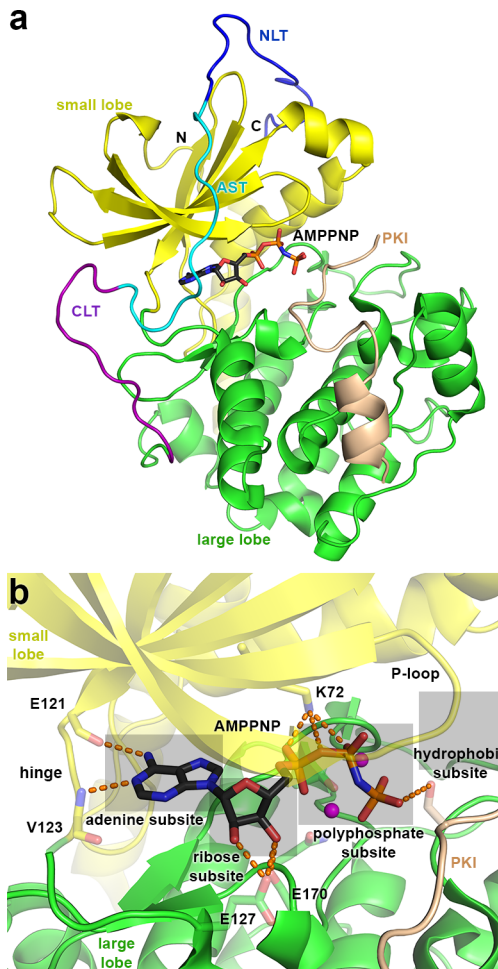


**Figure 1.** Overview of the catalytic subunit of PKA, the canonical AGC kinase. (a) The large (C) lobe (green) and small (N) lobe (yellow) of the kinase domain form the active site at their interface. The C-terminal extension of the domain, characteristic of AGC kinases, extends from the C-terminus of the large lobe, passes over the active site, and then interacts with the small lobe. Three regions of the extension have been described as the C-lobe tether (CLT, purple), the active site tether (AST, cyan), and the N-lobe tether (NLT, blue).<sup>37</sup> In this structure, a peptide substrate (colored wheat) was cocrystallized with the enzyme in complex with an AMPPNP substrate analogue (stick model; PDB entry 4HPU). The amino and carboxyl termini of the domain are labeled N and C, respectively. (b) Close-up view of AMPPNP bound in the active site of PKA illustrates the adenine, ribose, and polyphosphate subsites commonly occupied by kinase inhibitors.<sup>36</sup> A fourth hydrophobic subsite is sometimes occupied by larger inhibitors such as balanol and the Takeda compounds.<sup>77,80</sup> Hydrogen bonds formed between the adenine ring of AMPPNP and the hinge, ribose and the large lobe, and catalytic lysine are shown as dashed lines. These hydrogen bonds are often recapitulated in small molecule inhibitor complexes.

N-lobe tether (NLT), which packs against the small lobe of the kinase domain and often contributes an extra helix and  $\beta$  strand to the domain (Figure 1a).<sup>37</sup> PDK1 interacts in *trans* with the NLT of other AGC kinases and activates them via transphosphorylation of their activation loops.<sup>38</sup> The AST is not only one of the most flexible regions of the AGC kinase domain but also one of the most variable in sequence,<sup>37</sup> making it difficult to resolve in crystal structures and to homology model. However, given that residues in the AST can form direct interactions with ligands in the active site cleft, it also likely

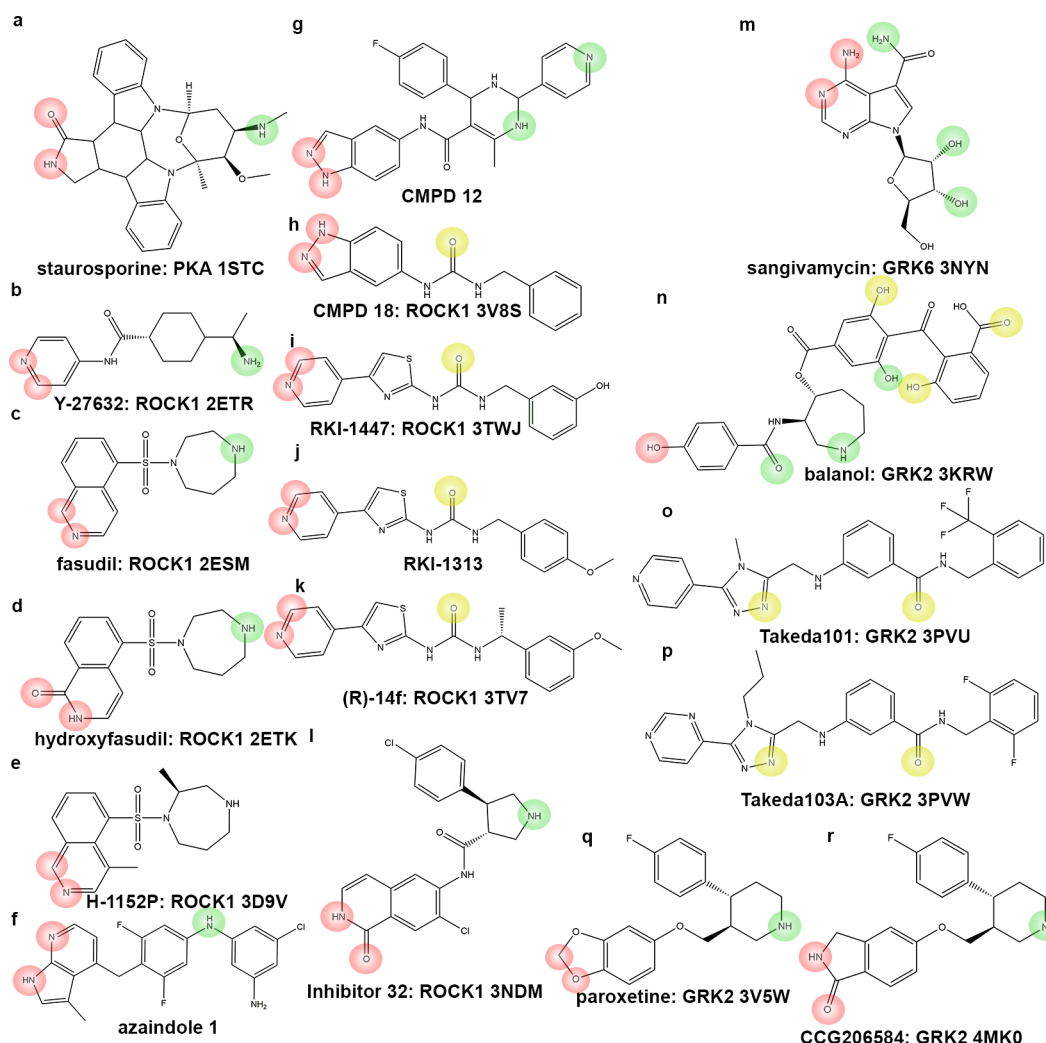


**Figure 2.** Structure of small molecule AGC kinase inhibitors. Hydrogen bonds formed by these compounds in crystal structures (indicated by PDB ID and target kinase where applicable) or predicted by homology models are highlighted with spheres: hydrogen bonds with the hinge are shown in red, those with the large lobe are shown in green, and those with the small lobe are shown in yellow.

contributes to the specificity and affinity of some inhibitors. The structure of the AST region, in combination with the relative orientation of the small and large lobes, is thus an important consideration for the rational design of drugs that selectively target AGC kinases.

## ■ SMALL MOLECULE INHIBITION OF OTHER AGC KINASES

**Staurosporine.** The natural product staurosporine (Figure 2a) was initially identified as a potent inhibitor of PKC ( $IC_{50} = 2 \text{ nM}$ ).<sup>39</sup> However, even in this initial report it was noted that staurosporine exhibits comparable inhibition of PKA and is now known as an efficacious inhibitor of many protein kinases. The crystal structure of staurosporine in complex with PKA<sup>40</sup> (Figure 3) demonstrated that it binds in the ATP binding site despite exhibiting a noncompetitive mechanism of inhibition.<sup>41</sup> The large aromatic ring system of staurosporine drives the two lobes of the kinase domain into a conformation slightly more open than the activated state, as it does when in complex with PKC,<sup>42</sup> p90 ribosomal S6 kinase (RSK),<sup>43</sup> and PDK1.<sup>44</sup> The buried accessible surface area (ASA) for staurosporine bound to PKA is considerably higher than that of AMPPNP (330 vs 225

$\text{\AA}^2$ , respectively), which likely underlies their difference in inhibitory potency (Table 1).

Staurosporine exploits features that are common to all protein kinase active sites. In the adenine subsite, the lactam group of staurosporine binds in the same planar pocket and makes specific contacts analogous to those of the adenine ring of ATP. For example, in the PKA complex, the cyclic nitrogen and carbonyl oxygen of the lactam form hydrogen bonds with the backbone carbonyl of Glu121 and the amide nitrogen of Val123, respectively, in the hinge of the kinase domain (Figure 3). In the ribose binding site, staurosporine forms an additional hydrogen bond with the same backbone carbonyl (Glu170 in PKA), as would the 3'-OH of ribose.

The interactions of promiscuous drugs like staurosporine highlight some of the challenges in designing selective protein kinase inhibitors. The structure of the ATP binding pocket is increasingly similar as different kinase domains adopt increasingly active conformations, and specific hydrogen bonds are typically formed between the drug and the peptide backbone or invariant residues. Slight alteration in the relative orientation of the small and large lobes helps to alleviate any steric clashes that might arise due to the presence of unique side chains in the active site of one kinase versus another.

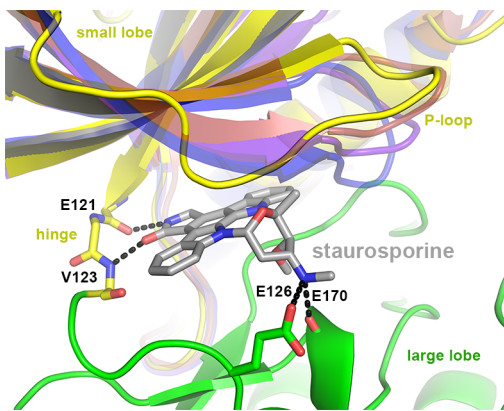


**Figure 3.** Staurosporine forms hydrogen bonds with elements conserved among many AGC kinase active sites but allows for multiple P-loop conformations. The view is essentially the same as that in Figure 1b. Staurosporine (gray carbons) binds in nearly superimposable conformations in PKA (yellow small lobe and green large lobe, PDB ID: 1STC), PKC $\theta$  (blue, PDB ID: 1XJD), RSK1 (purple, PDB ID: 2Z7R), and PDK1 (red, PDB ID: 1OKY). The same hydrogen bonds (black dashed lines) with backbone atoms or conserved side chains are formed in each complex (PKA numbering). However, the P-loop exhibits either open (PKA and PDK1) or closed conformations (PKC $\theta$  and RSK1). The AST loop is omitted for clarity. Residue numbers correspond to those of PKA.

Consequently, the development of selective AGC kinase inhibitors generally requires deemphasizing the formation of specific interactions and instead focusing on trapping conformations unique to individual kinases<sup>36</sup> or on interactions

with unique features outside the canonical active site, such as the AST region. However, it should be noted that although staurosporine traps AGC kinases in very similar closed conformations, a wide variety of P-loop conformations are observed in these structures (Figure 3), perhaps because it is influenced by less conserved residues outside the active site. Thus, even highly conserved active site elements can still be exploited to confer additional selectivity so long as they are sufficiently flexible.

**ROCK Inhibitors.** Despite the high homology of AGC kinase active sites, highly potent and selective small molecule inhibitors have been identified for specific subfamilies. Of particular interest with respect to GRKs is the Rho-associated coiled-coil containing kinase subfamily (ROCK1 and ROCK2), which is a therapeutic target due to its roles in regulating cell migration and smooth muscle relaxation.<sup>45–47</sup> ROCKs and GRKs share a number of atypical features among AGC kinases that may avail them to the design of selective drugs. The first is that they do not require phosphorylation of their activation loops to achieve a fully active state. Accordingly, crystal structures demonstrate that the catalytic residues of the individual small and large lobes are well-ordered and in an active configuration. This likely reflects that the fact that the key activation event for these enzymes is the binding of regulatory proteins that coerce the kinase domain to close into a catalytically competent configuration. In the case of ROCK, it requires the binding of activated RhoA to its coiled-coil domain, whereas for GRKs, it requires the binding of an activated GPCR. Thus, the conformation of the active site cleft of these enzymes in their inactive states is likely quite different from those of other AGC kinases. Second, ROCK1 has a

**Table 1. Properties of PKA•, ROCK1•, and GRK2•Inhibitor Complexes**

complex	PDB ID	buried ASA ( $\text{\AA}^2$ ) <sup>c,g</sup>	potency (nM)	no. H bonds
PKA·2Mg <sup>2+</sup> ·AMPPNP <sup>a</sup>	4HPU	240	0.2 <sup>h</sup>	11
PKA·staurosporine <sup>a</sup>	1STC	330	8 <sup>i</sup>	3
PKA·balanol <sup>b</sup>	1BX6	420	4 <sup>j</sup>	7
PKA-Y-27632 <sup>a</sup>	1Q8T	235 <sup>f</sup>	25 000 <sup>k</sup>	2 <sup>j</sup>
PKA-fasudil <sup>a</sup>	1Q8W	235	460 <sup>k</sup>	3
PKA-hydroxyfasudil <sup>a</sup>	2ERZ	235	2200 <sup>k</sup>	3
PKA-H-1152P <sup>c</sup>	1Q8U	245	630 <sup>k</sup>	2(1) <sup>t</sup>
ROCK1-Y-27632 <sup>a</sup>	2ETR	210	140 <sup>k</sup>	3
ROCK1-fasudil <sup>a</sup>	2ESM	220	530 <sup>k</sup>	3
ROCK1-hydroxyfasudil <sup>a</sup>	2ETK	220–230 <sup>k</sup>	150 <sup>k</sup>	3
ROCK1-H-1152P <sup>c</sup>	3D9V	255	16 <sup>k</sup>	2(1)
ROCK1·RKI-1447 <sup>d</sup>	3TWJ	260–280	14 <sup>l</sup>	3(1)
ROCK1-(R)-14f <sup>b</sup>	3TV7	280–290	30 <sup>m</sup>	3(1)
ROCK1·cmpd 18 <sup>b</sup>	3V8S	245–250	650 <sup>n</sup>	3
ROCK1·inhibitor 32 <sup>b</sup>	3NDM	300–320	11 <sup>o</sup>	3
ROCK1·cmpd 22 <sup>b</sup>	3NCZ	245–260	15 <sup>p</sup>	3
GRK2·balanol <sup>b</sup>	3KRW	424	42 <sup>q</sup>	8
GRK2·paroxetine <sup>a</sup>	3VSW	246	5000 <sup>r</sup>	3(1)
GRK2-CCG206584 <sup>b</sup>	4MK0	272	2500 <sup>r</sup>	3
GRK2-Takeda101 <sup>b</sup>	3PVU	374	290 <sup>s</sup>	2
GRK2-Takeda103A <sup>b</sup>	3PVW	387	54 <sup>s</sup>	2

<sup>a</sup>Available commercially through many suppliers such as Sigma. <sup>b</sup>Likely requires isolation from *Verticillium balanoides*. <sup>c</sup>Available commercially through suppliers such as Enzo Life Sciences. <sup>d</sup>Available from AxonMedChem. <sup>e</sup>Buried accessible surface area (ASA) with the kinase domain, as calculated by the CCP4 program suite.<sup>85</sup> Excludes surfaces buried with residues from bound peptide substrate analogs in the PKA structures. <sup>f</sup>The ligand in this structure may be modeled incorrectly. If the aminoethyl group of the inhibitor is rotated so that it resembles other Y-27632 complexes in the PDB, then the ASA is 230  $\text{\AA}^2$  and the number of hydrogen bonds is 3. <sup>g</sup>Ranges indicate values calculated for independent chains in the asymmetric unit. <sup>h</sup> $K_D^{86}$  <sup>i</sup> $K_r^{40}$  <sup>j</sup> $K_r^{76}$  <sup>k</sup> $K_r^{50}$  <sup>l</sup> $IC_{50}^{54}$  <sup>m</sup> $IC_{50}^{55}$  <sup>n</sup> $IC_{50}^{53}$  <sup>o</sup>ROCK2,  $IC_{50}^{56}$  <sup>p</sup>ROCK2,  $IC_{50}^{57}$  <sup>q</sup> $IC_{50}^{77}$  <sup>r</sup> $IC_{50}^{82}$  <sup>s</sup> $IC_{50}^{80}$  <sup>t</sup>(Parentheses corresponds to an additional carbon–oxygen hydrogen bond to a backbone amide in the hinge of the kinase domain.

unique “signature” of side chains at positions that are variable in the active site: Ile82, Met156, Asp160, and Ala215 in the kinase domain and Phe368 in the AST.<sup>48</sup> GRKs have a nearly identical active site signature in the kinase domain: Ile197, Met274, Asp278, and Ser334 (GRK2 numbering). GRK2-Ala484 in the AST region is not structurally equivalent to ROCK1-Phe368, but it likewise makes contacts with ligands in the active site.<sup>49</sup> Thus, it stands to reason that if one can develop potent inhibitors of ROCKs that are selective versus most other AGC kinases, then one should be able to develop potent and selective inhibitors of GRKs. Taking advantage of the distinct signature residue in the GRK active site (GRK2-Ser334) may be key to developing compounds that are selective for GRKs over ROCKs. Thus, it is important to understand how known ROCK inhibitors interact with and are affected by substitutions at this position.

The most rigorous evaluation of how ROCK selectivity is achieved was performed by comparing atomic structures of the pyridine containing inhibitor Y-27632 and an isoquinoline inhibitor series represented by fasudil, hydroxyfasudil, and H-1152P (Figure 2b–e, respectively) in complex with ROCK1<sup>50</sup> with those of the same compounds in complex with PKA.<sup>50,51</sup> H-1152P is the most potent ( $K_i = 6$  nM) and selective for ROCK1 (50–500-fold). Y-27632, although less potent ( $K_i = 150$  nM), is also highly selective (>30-fold), whereas fasudil is not selective. All four inhibitors make similar hydrogen bonds with the kinase domain hinge via their aromatic pyridine or isoquinoline rings, which bind in the adenine subsite (Figure 4a). The remainder of each inhibitor occupies the ribose subsite, but none recapitulates the hydrogen bond formed by the 3'-OH of ATP. One of the most important conclusions from these comparisons is that the smaller Ala215 signature residue in ROCK1, analogous to Thr183 in PKA, allows inhibitors to bind deeper in the ROCK1 active site cleft, resulting in a ~7° change in orientation from the PKA-bound structure.<sup>50</sup> Interestingly, fasudil, which inhibits ROCK1 and PKA equally well, adopts a distinct conformation in each complex due to different modes of interaction with signature position ROCK1-Asp60/PKA-Glu127.

Even more potent and selective inhibitors of ROCKs have been reported that exploit other conserved features of the AGC kinase active site. Azaindole-1 (Figure 2f) is very potent inhibitor of ROCK1 and ROCK2 ( $IC_{50} = 0.6$  nM and 1.1 nM, respectively).<sup>48</sup> When evaluated against a panel of over 100 other kinases, only a few receptor tyrosine kinases showed significant inhibition. Modeling suggests that in addition to the expected hinge interactions the compound likely forms specific contacts with ROCK1-Asp160 and -Asp202. A series of inhibitors consisting of an indazole group amide linked to a series of dihydropyrimidines has been shown to have high potency ( $IC_{50} = 5$  nM) and >200-fold selectivity over evaluated related kinases such as RSK1.<sup>52</sup> The crystal structure of one of these derivatives (compound 12, Figure 2g) in complex with ROCK1 revealed that the flat aromatic indazole ring forms the expected hydrogen bonds with the hinge in the adenine subsite, whereas the dihydropyrimidine occupies the ribose subsite and forms a hydrogen bond with Asn203, a residue that contributes to  $Mg^{2+}$  coordination in the kinase-ATP complex. A hydrogen bond with the side chain of catalytic Lys200 was also postulated to increase binding affinity. Another series of indazole containing compounds led to the identification of compound 18 (Figure 2h) that exhibits 650 nM potency against ROCK1 and ROCK2.<sup>53</sup> The *in vitro* selectivity of this compound was

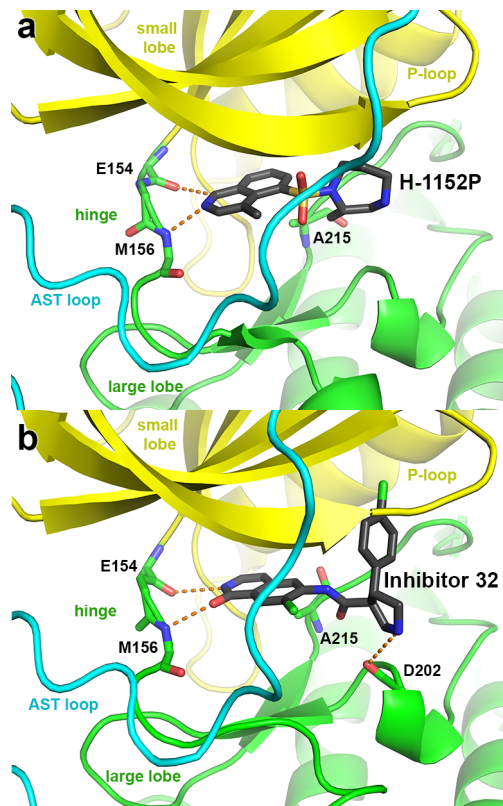


**Figure 4.** Structures of ROCK1 in complex with selected small molecule inhibitors. (a) ROCK1 (small lobe yellow and large lobe green) in complex with H-1152P (black carbons), which forms one conventional and one carbon–oxygen hydrogen bond (orange dashed lines) with the hinge of the kinase domain in the adenine subsite (PDB ID: 3D9V). (b) The ROCK1-inhibitor 32 complex (PDB ID: 3NDM) incorporates an additional hydrogen bond with the main chain carbonyl of Asp202 in the ribose subsite and occupies the polyphosphate subsite with a *p*-chlorophenyl ring. Other ROCK1 and GRK2 inhibitors commonly exhibit analogous interactions.

not reported, but it did not inhibit the phosphorylation of non-ROCK substrates in cancer cells. Unlike compound 12 above, compound 18 extends a phenyl ring into a pocket in the polyphosphate subsite formed between the P-loop and the aliphatic portion of the active site Lys105. A drug series based on a pyridylthiazole scaffold led to the discovery of RKI-1447 (Figure 2i) and RKI-1313 (Figure 2j) ( $IC_{50} = 14.5$  and 6.2 nM, respectively)<sup>54</sup> and of compound (R)-14f (Figure 2k) ( $IC_{50} = 30$  nM),<sup>55</sup> which also exhibit high selectivity. Their pyridine rings form the expected hydrogen bond with the hinge as observed for Y-27632, and their terminal *meta*-hydroxy or *ortho*-methoxy phenyl rings bind in the polyphosphate subsite much like the phenyl group of compound 18. Potent 2*H*-isoquinolin-1-one containing compounds bind to the hinge in a manner similar to hydroxyfasudil,<sup>56,57</sup> and one such compound (inhibitor 32;  $IC_{50} = 11$  nM, Figure 2l) has a *para*-chlorophenyl group that docks into the polyphosphate binding site in a manner similar to that of compound 18, RKI-1447, RKI-1313, and (R)-14f. Thus, occupation of the polyphosphate binding pocket by a substituted phenyl is another commonly observed feature among ROCK inhibitors.

The publically available crystal structures of ROCK-inhibitor complexes along with their buried accessible surface area (ASA) and reported inhibition constants are listed in Table 1. Examination of their properties leads to several conclusions.

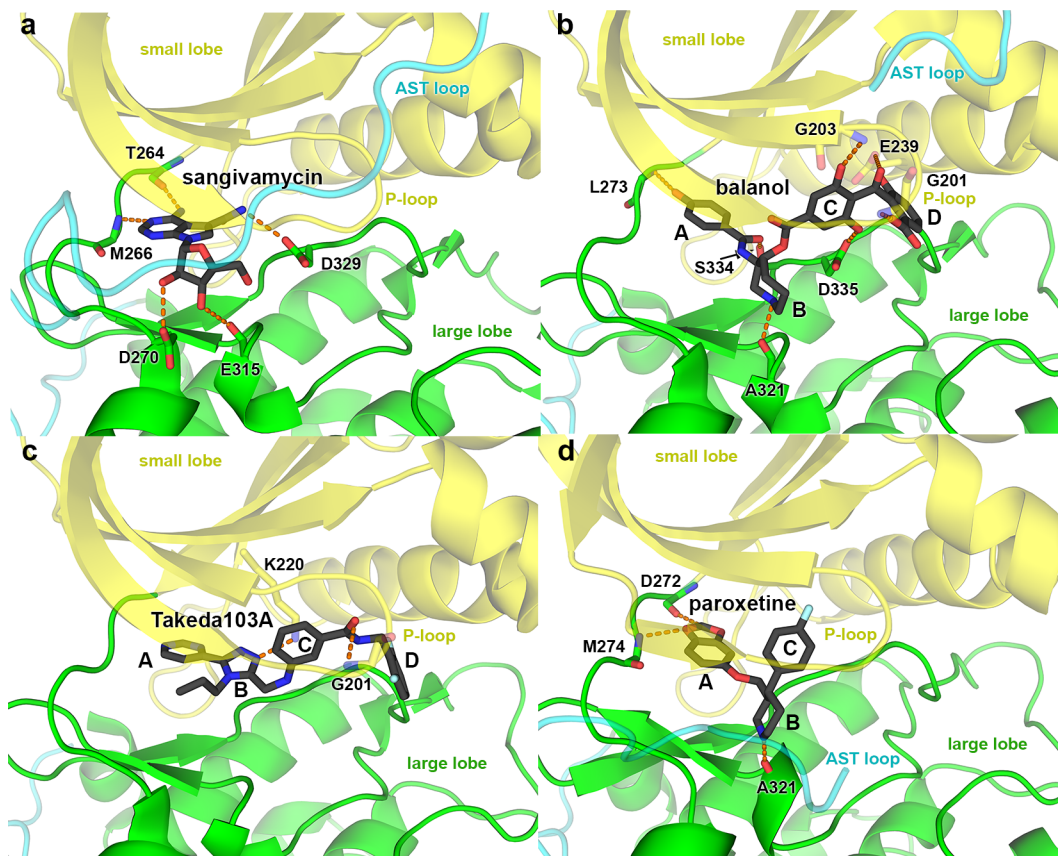


**Figure 5.** GRKs in complex with small molecule inhibitors: (a) GRK6-sangivamycin, (b) GRK2-balanol, (c) GRK2-Takeda103A, and (d) GRK2-paroxetine. Each GRK is shown in a similar orientation. Inhibitors are shown as stick models with black carbons. The A, B, C, and D rings of balanol, Takeda103A, and paroxetine are labeled A–D, if present. These chemical groups occupy the adenine, ribose, polyphosphate, and hydrophobic subsites, respectively, with the B ring exhibiting the most divergence in structure. The AST loop of the C-terminal extension (semitransparent cyan) is most ordered in the GRK6-sangivamycin complex, but it is also relatively well ordered in the GRK2-paroxetine complex, which is believed to adopt a conformation analogous to that of a product complex. These GRK2 structures feature a kinase domain with a more closed conformation than that observed in the balanol and Takeda103A complexes. Note the strong structural similarity of paroxetine with inhibitor 32 in Figure 4b.

As noted previously,<sup>50,51</sup> there is a rough correlation between potency of inhibition and total buried surface area but not with the number of hydrogen bonds. This correlation is strongest when examining a series of inhibitors against the same protein kinase. The most potent inhibitors are typically those that bury  $>250 \text{ \AA}^2$  of accessible surface area. Some of the most selective, e.g. H-1152P, make only a few strong hydrogen bonds with the protein. These molecular principles are likely equally important for the development of potent and selective GRK2 inhibitors.

## ■ NON-DRUG-LIKE INHIBITORS OF GRKS

Early studies of GRKs examined their inhibition by highly charged molecules. Polycations such as spermine ( $\text{IC}_{50} = 990 \mu\text{M}$ ), spermidine ( $\text{IC}_{50} = 2.6 \text{ mM}$ ), and polylysine ( $\text{IC}_{50} = 69 \mu\text{M}$ ) inhibit GRK2 weakly, but anionic compounds such as heparin and dextran sulfate show much greater potency ( $\text{IC}_{50} = 0.15 \mu\text{M}$ ). Inhibition by anionic compounds could be counteracted through the addition of cations, suggesting that the underlying mechanism is electrostatic neutralization.<sup>58</sup> Indeed, it is likely that polyanions mask highly basic regions of GRK2 that are necessary for beneficial interactions with the cell membrane or that line the basic polypeptide binding groove on the large lobe.<sup>59</sup> However, such highly charged, membrane-impermeable molecules hold little promise for therapeutic development.

Peptide inhibitors derived from the first intracellular loop of the hamster  $\beta_2$ -AR exhibit  $\text{IC}_{50}$  values as low as  $40 \mu\text{M}$  for GRK2, and sequence optimization decreased these values to  $600 \text{ nM}$ .<sup>60,61</sup> However, even the most potent of these peptides has poor selectivity over GRK3 ( $2.6 \mu\text{M}$ ) or GRK5 ( $1.6 \mu\text{M}$ ). Interestingly, these peptides are noncompetitive for both receptors and ATP,<sup>61</sup> which suggests that they may not be targeting the GPCR binding site of these GRKs as originally intended. This theory is consistent with the fact that most residues in the first intracellular loop of the activated  $\beta_2$ -AR are not available for intermolecular contacts.<sup>3</sup> Regardless, expression of the optimized peptide is capable of inhibiting GRK-dependent cointernalization of heterodimers of the angiotensin-1 and bradykinin-2 receptors,<sup>62</sup> and the peptide can promote tumor growth, suggesting that stimulation of growth pathways may be part of the cardioprotective effects observed for GRK2 inhibition.<sup>62,63</sup> Another peptide inhibitor study investigated the ability of a set of peptides derived from helices 3, 9, and 10 of GRK5, the  $\alpha 9$  helix of GRK5/6, and the carboxyl terminal tail of transducin to inhibit GRK2, GRK5, GRK6, and GRK7.<sup>64,65</sup> Greater than 50% inhibition was measured at  $100 \mu\text{M}$  concentrations of each peptide, but, like the hamster  $\beta_2$ -AR derived peptides, they exhibit low selectivity among GRKs.

An RNA aptamer (C13) potently inhibits GRK2 ( $\text{IC}_{50} = 4 \text{ nM}$ ) with 20-fold selectivity over GRK5 and nearly

undetectable inhibition of other evaluated protein kinases, including the AGC kinases AKT1 and ROCK2.<sup>66</sup> The crystal structure of a truncated variant of the aptamer in complex with GRK2 and G $\beta\gamma$  (PDB ID: 3UZT)<sup>67</sup> revealed that an adenine nucleotide in a hairpin loop of the RNA aptamer binds in the active site in a manner that mimics the substrate ATP. Other regions of the aptamer make extensive interactions with the large lobe of the kinase domain, remodeling basic regions of the protein so that they can better interact with the polyanionic phosphodiester backbone of the RNA. Because the affinity of the aptamer was reduced substantially at high ionic strength, the manner in which the RNA aptamer binds the large lobe of GRK2 could be representative of the mechanism of inhibition by polyanions such as heparin.

## ■ SMALL MOLECULE GRK2 INHIBITORS

The drugs tamoxifen and chloropromazine have been reported to inhibit GRK2 with IC<sub>50</sub> values ranging from 30 to 45  $\mu\text{M}$ , but these compounds are unlikely candidates for GRK inhibitor design due to their strong inhibition of other targets.<sup>68</sup> In another report, low-potency, but reasonably selective, inhibitors of GRK2 were rationally designed (IC<sub>50</sub> = 125–500  $\mu\text{M}$ ).<sup>69</sup> A more recent study reported development of a molecule (compound 1o) that has IC<sub>50</sub> values of 460 and 59 nM for GRK2 and GRK5, respectively, as measured using a time-resolved fluorescence resonance energy transfer assay.<sup>70</sup> However, none of these inhibitors have yet been structurally characterized in complex with a GRK and thus their mechanisms of action are unknown.

The cancer chemotherapeutic sangivamycin (Figure 2m) is a potent GRK inhibitor with  $K_i$  values ranging from 0.2–10  $\mu\text{M}$  (J. Tesmer, unpublished data).<sup>71</sup> However, like many other adenine nucleoside analogues, it is a promiscuous inhibitor that inhibits other AGC kinases such as PKC<sup>72</sup> and nonserine/threonine kinases such as the epidermal growth factor receptor.<sup>73</sup> Sangivamycin was crystallized in complex with GRK6<sup>74</sup> and, not surprisingly, binds in the active site in the same manner as that of the adenosine moiety of the substrate ATP (Figure 5a). Interestingly, the GRK6 kinase domain in this complex adopts the most active conformation yet reported for a GRK, and its AST region is well-ordered. The amide group at the C7 position of the diazaindole ring of sangivamycin forms van der Waals contacts with the gatekeeper residue (GRK6-Leu263) and may form a weak hydrogen bond with the side chain of GRK6-Asp329. Otherwise, the inhibitor binds in a manner similar to how fasudil binds ROCK1 (Figure 2c).

The natural product balanol (Figure 2n) consists of four ring systems (A–D) attached in a linear manner and inhibits many AGC kinases with nanomolar potency.<sup>75,76</sup> Interestingly, balanol exhibits 50- and 100-fold selectivity for GRK2 over GRK5 and GRK1, respectively.<sup>77</sup> Crystal structures of balanol in complex with PKA and GRK2 have been reported,<sup>77,78</sup> and both illustrate a similar largely extended conformation for the compound in the active site (Figure 5B). The A and B rings of balanol bind in the adenine and ribose subsites, respectively, whereas the aromatic C ring binds to the polyphosphate subsite in a manner highly reminiscent of the phenyl ring of compound 18 (Figure 2h). The D ring extends into the hydrophobic subsite. The hydroxyl of the A ring of balanol forms two hydrogen bonds with the hinge of the kinase domain. The azepane B ring makes a hydrogen bond to the backbone carboxyl of GRK2-Ala321 (GRK2), mimicking the hydrogen bond formed by the 3'-OH of ATP. The amide linkage

between the A and B rings forms a hydrogen bond with signature residue GRK2-Ser334. The C-ring forms hydrogen bonds with a backbone nitrogen in the P-loop and with GRK2-Asp335. Two more hydrogen bonds are formed by the D ring with a backbone amide of the P-loop and the side chain of Glu239 (Table 1). As in the case of staurosporine, these hydrogen bonds involve backbone atoms or side chains conserved across all AGC kinases, likely contributing to the relatively poor selectivity of the drug. Balanol stabilizes a conformation of the kinase domain of GRK2 that closely resembles what is believed to be the apo state of GRK2 (Figure 5b).<sup>77</sup> Via docking studies, it was conjectured that less optimal contacts made by the A ring of balanol and by unconserved positions in the active site accounts for its lower potency against GRK1 and GRK5.

Two closely related compounds identified by Takeda Pharmaceuticals Inc. (101 and 103A, Figure 2o,p) exhibit similar potency of inhibition against GRK2 as that of balanol (Table 1), but they have dramatically better selectivity for GRK2 over other GRKs and AGC kinases (IC<sub>50</sub> > 2  $\mu\text{M}$ ).<sup>79</sup> The conformation of the GRK2 kinase domain in complex with these compounds is very similar to that of GRK2 bound to balanol.<sup>80</sup> Like balanol, these molecules consist of four ring systems (A–D) attached in a linear fashion that occupy the adenine, ribose, polyphosphate, and hydrophobic subsites (Figure 5c). Their A, C, and D rings adopt similar orientations. Interestingly, the Takeda compounds only form van der Waals interactions with the hinge via their A rings. The B ring of the Takeda compounds is a methyl or propyl triazole that packs closely against the small lobe of the kinase domain, essentially where the  $\alpha$ -phosphate of ATP would bind, forming a hydrogen bond with the side chain of Lys220. The methyl or propyl group fills the rest of the ribose subsite. The triazole ring also forms close contacts to the side chain of GRK2-Ser334, one of the signature residues. Despite structural differences in the D rings of the two Takeda compounds and balanol, the conformation of residues bounding this site (Phe202, Leu235, Leu338) is similar in each complex, and the D ring of each inhibitor is poorly ordered, suggesting high mobility in this pocket. These compounds form only two obvious hydrogen bonds, one with Lys220 and another with the P-loop, far fewer than that of balanol. Potency of inhibition by the Takeda compounds was insensitive to site-directed mutagenesis of active residues that differ among GRKs.<sup>80</sup> Thus, the selectivity of these compounds for GRK2 may be dictated primarily by the unique open, inactive conformation of its kinase domain that may increase buried surface area or, alternatively, avoid steric clashes that may occur in the apo conformations favored by other GRK subfamilies. The fact that the Takeda compounds do not form the stereotypical hinge interactions may also contribute to selectivity. Despite the ability of Takeda compounds 101 and 103A to augment cardiac inotropy,<sup>79</sup> to date there has been no further information reported on them, suggesting that they have undesirable qualities that preclude advancement to clinical trials.

The selective serotonin reuptake inhibitor paroxetine (Figure 2q) was identified as part of a high-throughput screen that measured the ability of small molecules to displace a fluorescently tagged version of the C13 aptamer.<sup>49,81</sup> Although the screen had the potential to identify ligands that bind outside the active site, paroxetine was shown to bind directly in the orthosteric site.<sup>49</sup> Paroxetine is a much less potent inhibitor than balanol or the Takeda compounds, with IC<sub>50</sub> values

ranging from 5 to 20  $\mu\text{M}$ ,<sup>49,82</sup> depending on the assay conditions. However, it exhibits selectivity for GRK2 over GRK1 (16–60-fold) and GRK5 (13–50-fold). Paroxetine also has an approximately 10- and 40-fold selectivity for GRK2 over PKA and PKC, respectively.<sup>82</sup> The drug exhibits a number of striking structural similarities to some of the ROCK inhibitors described above, in particular compound 18 (Figure 2h) and inhibitor 32 (Figure 2l). It has a relatively low molecular weight, a large planar ring system that binds in the adenine subsite, and a *para*-fluorophenyl group that docks in the polyphosphate subsite (Figure 5d). Like the ROCK inhibitors, it traps the GRK2 kinase domain in a relatively closed conformation that results in partial ordering of the GRK2 AST, which forms van der Waals contacts with the piperidine B ring of the drug. Otherwise, the manner in which the drug binds is very similar to that of the A–C rings of balanol (Figure 5b). Like some of the ROCK inhibitors, the benzodioxole ring of paroxetine forms one conventional and one carbon–oxygen hydrogen bond with the hinge, although the carbon–oxygen hydrogen bond of paroxetine is expected to be much stronger based on its distance of 2.8 Å. The piperidine ring of paroxetine makes the analogous hydrogen bond to the large lobe as that of the azepane ring of balanol. Paroxetine does not occupy the hydrophobic subsite, which may partially explain its lower affinity compared to that of balanol and the Takeda compounds. Because the  $K_D$  of paroxetine for GRK1, GRK2, and GRK5 is statistically the same and the structure of the active site in the GRK1-paroxetine complex is essentially the same as that of GRK2-paroxetine, the main driver of selectivity of paroxetine among GRKs seems to be the lower affinity of GRK2 for adenine nucleotides.<sup>82</sup>

Paroxetine is an FDA-approved drug that has excellent pharmacokinetic and pharmacodynamic properties. It has been shown to penetrate HEK293 cells, where it mediates GRK2-specific inhibition of thyrotropin-releasing hormone receptor, and to increase myocardial contractility in isolated mouse cardiomyocytes and whole animals.<sup>49</sup> Optimization of this scaffold to develop more potent and selective GRK inhibitors can hopefully preserve some of these qualities. A first attempt at rational design involved creating a benzolactam derivative of paroxetine (CCG-206584, Figure 2r) that can form two conventional hydrogen bonds with the hinge. Although structural analysis confirmed formation of these bonds, the inhibitor exhibited only mildly enhanced potency for GRK2 and exhibited less selectivity relative to PKA and PKC.<sup>82</sup> This result is consistent with the ideas that additional hydrogen bonds do not necessarily increase potency (Table 1), perhaps because of water desolvation effects, and that fewer hydrogen bonds with the hinge seems to be a route to higher selectivity.

## CONCLUSIONS

There has recently been great progress in the identification, development, and structural characterization of potent and selective AGC kinase inhibitors. These efforts provide a starting point for the development of increasingly selective and potent inhibitors of individual AGC kinase subfamilies that could ultimately lead to the rational design of useful therapeutics. Already, fasudil is clinically approved in Japan for treatment of cerebral vasospasm, and the staurosporine analogue ruboxistaurin is in clinical trials for the treatment of diabetic retinopathy.<sup>83</sup> The pursuit of highly potent, selective GRK inhibitors is likewise well underway, but increases in potency and selectivity are still required. Identification of the Takeda

compounds proves that nanomolar potency and high selectivity for GRK2 can be achieved, as has also been demonstrated for ROCKs.

Our analysis of the properties and interactions of ROCK and GRK inhibitors suggests several design principles that may lead to higher selectivity and potency. Many of the ROCK and GRK inhibitors characterized structurally thus far contact the hinge with the edge of a planar, usually aromatic ring system that binds in the same orientation as that of the adenine ring of ATP. Two conventional hydrogen bonds with the hinge seem to decrease selectivity, as some of the most selective compounds either lack both hydrogen bonds or exhibit weaker interactions (e.g., paroxetine and the Takeda compounds for GRK2, and H-1152P for ROCK1). One explanation for this phenomenon could be that drugs with less specific or more flexible hinge interactions will have greater latitude to complement other features in the active site that may be specific to individual protein kinases, leading to increased buried surface area. These unique features may result from a distinct relative orientation of the small and large lobes, from unique side chains in the active site signature, or from the contribution of residues in the highly variable AST region. There is considerable divergence in how the inhibitors occupy the ribose subsite, although many of them form a hydrogen bond analogous to that formed by the 3'-OH of ATP. Because the chemical groups that occupy this subsite have been shown to interact with residues in the AST region, which is highly divergent even among GRKs, modifications here could be exploited to increase selectivity. Indeed, PKA, but not PKC, is sensitive to balanol derivatives with changes in the chemical structure of the B ring.<sup>84</sup> The polyphosphate subsite interactions are strikingly similar among ROCK and GRK inhibitors and thus it does not seem to be a subsite where selectivity among AGC kinases can be dramatically improved. However, occupation of this site clearly strongly contributes to potency. Finally, inhibitors that occupy the hydrophobic subsite, such as balanol and the Takeda compounds, are among the most potent against GRK2, but it remains to be seen if differences in this site can be exploited to achieve selectivity among GRKs. This is definitely the case for some AGC kinases. For example, removal of the carboxylate group from the benzophenone D ring of balanol led to over 2000-fold selectivity for PKA over PKC without significantly changing potency of inhibition versus PKA.<sup>84</sup> The molecular basis for why loss of this carboxylate leads to such a dramatic loss of potency against PKC is not clear, but it was proposed that sequence differences in the AST and  $\alpha$ B helix near the hydrophobic subsite could play a role. The fact that ROCK1 and 2 have a phenylalanine side chain (ROCK1-Phe120) that partially occupies the hydrophobic subsite suggests that inhibitors that occupy this subsite will select against ROCKs. This idea remains to be tested. Finally, because GRKs have a serine (GRK2-Ser334) in their active site signature instead of alanine in ROCKs or threonine in most other AGC kinases, interactions with this residue could also be exploited to gain selectivity so long as the larger serine side chain does not prevent the inhibitors from maximizing their buried surface area.<sup>50</sup>

Structural and biochemical analysis suggests that inhibitor selectivity among GRKs is driven by a number of different factors. Perhaps the most important is the ability of the kinase domain to adopt a conformation that is compatible with the compound, as seems to be the case for the Takeda

compounds<sup>49</sup> because they interact with a conformation of GRK2 that has not yet been observed in other GRKs. Selectivity, when assessed via inhibition of phosphorylation, can also derive from differential affinities of these kinases for their substrates and products. Indeed, GRK2 binds ATP and ADP less tightly than does GRK1 or GRK5,<sup>82</sup> leading to more potent IC<sub>50</sub> values of paroxetine against GRK2.

In summary, it is now clear that selective inhibitors with nanomolar potency for GRKs can be identified. These compounds bear many similarities to ROCK1 and 2 inhibitors. Furthermore, GRK inhibitors can have both desirable drug-like properties and high selectivity. Future generations of rational design are expected to lead to the development of even more selective chemical probes that can be used to deconvolute GRK function in cells, where multiple GRKs are expressed, and of drugs that could be used to treat heart failure and other GRK-dependent pathophysiological conditions.

## AUTHOR INFORMATION

### Corresponding Author

\*E-mail: tesmerjj@umich.edu.

### Notes

The authors declare no competing financial interest.

## ACKNOWLEDGMENTS

This work was supported by National Institutes of Health grant nos. HL071818 and HL086865 (J.J.G.T.) and American Heart Association grant no. N014938 (K.T.H.).

## REFERENCES

- (1) Moore, N. A., Tye, N. C., Axton, M. S., and Risius, F. C. (1992) The behavioral pharmacology of olanzapine, a novel “atypical” antipsychotic agent. *J. Pharmacol. Exp. Ther.* 262, 545–551.
- (2) Tattersfield, A. E., and McNicol, M. W. (1969) Salbutamol and isoproterenol. A double-blind trial to compare bronchodilator and cardiovascular activity. *N. Engl. J. Med.* 281, 1323–1326.
- (3) Rasmussen, S. G., DeVree, B. T., Zou, Y., Kruse, A. C., Chung, K. Y., Kobilka, T. S., Thian, F. S., Chae, P. S., Pardon, E., Calinski, D., Mathiesen, J. M., Shah, S. T., Lyons, J. A., Caffrey, M., Gellman, S. H., Steyaert, J., Skiniotis, G., Weis, W. I., Sunahara, R. K., and Kobilka, B. K. (2011) Crystal structure of the  $\beta_2$  adrenergic receptor-Gs protein complex. *Nature* 477, 549–555.
- (4) Cherezov, V., Rosenbaum, D. M., Hanson, M. A., Rasmussen, S. G., Thian, F. S., Kobilka, T. S., Choi, H. J., Kuhn, P., Weis, W. I., Kobilka, B. K., and Stevens, R. C. (2007) High-resolution crystal structure of an engineered human  $\beta 2$ -adrenergic G protein-coupled receptor. *Science* 318, 1258–1265.
- (5) Kruse, A. C., Hu, J., Pan, A. C., Arlow, D. H., Rosenbaum, D. M., Rosemond, E., Green, H. F., Liu, T., Chae, P. S., Dror, R. O., Shaw, D. E., Weis, W. I., Wess, J., and Kobilka, B. K. (2012) Structure and dynamics of the M3 muscarinic acetylcholine receptor. *Nature* 482, 552–556.
- (6) Nickols, H. H., and Conn, P. J. (2014) Development of allosteric modulators of GPCRs for treatment of CNS disorders. *Neurobiol. Dis.* 61, 55–71.
- (7) Wisler, J. W., Xiao, K., Thomsen, A. R., and Lefkowitz, R. J. (2014) Recent developments in biased agonism. *Curr. Opin. Cell Biol.* 27C, 18–24.
- (8) Sjogren, B., Blazer, L. L., and Neubig, R. R. (2010) Regulators of G protein signaling proteins as targets for drug discovery. *Prog. Mol. Biol. Transl. Sci.* 91, 81–119.
- (9) Pearce, L. R., Komander, D., and Alessi, D. R. (2010) The nuts and bolts of AGC protein kinases. *Nat. Rev. Mol. Cell Biol.* 11, 9–22.
- (10) Gurevich, E. V., Tesmer, J. J., Mushegian, A., and Gurevich, V. V. (2012) G protein-coupled receptor kinases: more than just kinases and not only for GPCRs. *Pharmacol. Ther.* 133, 40–69.
- (11) Gurevich, V. V., and Gurevich, E. V. (2014) Extensive shape shifting underlies functional versatility of arrestins. *Curr. Opin. Cell Biol.* 27, 1–9.
- (12) Tilley, D. G. (2011) G protein-dependent and G protein-independent signaling pathways and their impact on cardiac function. *Circ. Res.* 109, 217–230.
- (13) Lorenz, K., Lohse, M. J., and Quitterer, U. (2003) Protein kinase C switches the Raf kinase inhibitor from Raf-1 to GRK-2. *Nature* 426, 574–579.
- (14) Gainetdinov, R. R., Bohn, L. M., Walker, J. K., Laporte, S. A., Macrae, A. D., Caron, M. G., Lefkowitz, R. J., and Premont, R. T. (1999) Muscarinic supersensitivity and impaired receptor desensitization in G protein-coupled receptor kinase 5-deficient mice. *Neuron* 24, 1029–1036.
- (15) Metaye, T., Gibelin, H., Perdrisot, R., and Kraimps, J. L. (2005) Pathophysiological roles of G-protein-coupled receptor kinases. *Cell. Signalling* 17, 917–928.
- (16) Belmonte, S. L., and Blaxall, B. C. (2011) G protein coupled receptor kinases as therapeutic targets in cardiovascular disease. *Circ. Res.* 109, 309–319.
- (17) Dorn, G. W., 2nd. (2009) GRK mythology: G-protein receptor kinases in cardiovascular disease. *J. Mol. Med.* 87, 455–463.
- (18) Felder, R. A., Sanada, H., Xu, J., Yu, P. Y., Wang, Z., Watanabe, H., Asico, L. D., Wang, W., Zheng, S., Yamaguchi, I., Williams, S. M., Gainer, J., Brown, N. J., Hazen-Martin, D., Wong, L. J., Robillard, J. E., Carey, R. M., Eisner, G. M., and Jose, P. A. (2002) G protein-coupled receptor kinase 4 gene variants in human essential hypertension. *Proc. Natl. Acad. Sci. U.S.A.* 99, 3872–3877.
- (19) Gold, J. I., Gao, E., Shang, X., Premont, R. T., and Koch, W. J. (2012) Determining the absolute requirement of G protein-coupled receptor kinase 5 for pathological cardiac hypertrophy: short communication. *Circ. Res.* 111, 1048–1053.
- (20) Eschenhagen, T. (2008)  $\beta$ -Adrenergic signaling in heart failure—adapt or die. *Nat. Med.* 14, 485–487.
- (21) Ungerer, M., Bohm, M., Elce, J. S., Erdmann, E., and Lohse, M. J. (1993) Altered expression of  $\beta$ -adrenergic receptor kinase and  $\beta_1$ -adrenergic receptors in the failing human heart. *Circulation* 87, 454–463.
- (22) Ungerer, M., Parruti, G., Bohm, M., Puzicha, M., DeBlasi, A., Erdmann, E., and Lohse, M. J. (1994) Expression of  $\beta$ -arrestins and  $\beta$ -adrenergic receptor kinases in the failing human heart. *Circ. Res.* 74, 206–213.
- (23) Hata, J. A., Williams, M. L., and Koch, W. J. (2004) Genetic manipulation of myocardial beta-adrenergic receptor activation and desensitization. *J. Mol. Cell. Cardiol.* 37, 11–21.
- (24) Koch, W. J., Rockman, H. A., Samama, P., Hamilton, R. A., Bond, R. A., Milano, C. A., and Lefkowitz, R. J. (1995) Cardiac function in mice overexpressing the  $\beta$ -adrenergic receptor kinase or a  $\beta$ ARK inhibitor. *Science* 268, 1350–1353.
- (25) Raake, P. W., Vinge, L. E., Gao, E., Boucher, M., Rengo, G., Chen, X., DeGeorge, B. R., Jr., Matkovich, S., Houser, S. R., Most, P., Eckhart, A. D., Dorn, G. W., 2nd, and Koch, W. J. (2008) G protein-coupled receptor kinase 2 ablation in cardiac myocytes before or after myocardial infarction prevents heart failure. *Circ. Res.* 103, 413–422.
- (26) Rengo, G., Lympereopoulos, A., Zicarelli, C., Donniciacuo, M., Soltys, S., Rabinowitz, J. E., and Koch, W. J. (2009) Myocardial adenovirus serotype 6- $\beta$ ARKct gene therapy improves cardiac function and normalizes the neurohormonal axis in chronic heart failure. *Circulation* 119, 89–98.
- (27) Shah, A. S., White, D. C., Emani, S., Kypson, A. P., Lilly, R. E., Wilson, K., Glower, D. D., Lefkowitz, R. J., and Koch, W. J. (2001) *In vivo* ventricular gene delivery of a  $\beta$ -adrenergic receptor kinase inhibitor to the failing heart reverses cardiac dysfunction. *Circulation* 103, 1311–1316.
- (28) White, D. C., Hata, J. A., Shah, A. S., Glower, D. D., Lefkowitz, R. J., and Koch, W. J. (2000) Preservation of myocardial  $\beta$ -adrenergic receptor signaling delays the development of heart failure after myocardial infarction. *Proc. Natl. Acad. Sci. U.S.A.* 97, 5428–5433.

- (29) Laugwitz, K. L., Kronsbein, K., Schmitt, M., Hoffmann, K., Seyfarth, M., Schomig, A., and Ungerer, M. (1997) Characterization and inhibition of  $\beta$ -adrenergic receptor kinase in intact myocytes. *Cardiovasc. Res.* 35, 324–333.
- (30) Rockman, H. A., Chien, K. R., Choi, D. J., Iaccarino, G., Hunter, J. J., Ross, J., Lefkowitz, R. J., and Koch, W. J. (1998) Expression of a  $\beta$ -adrenergic receptor kinase 1 inhibitor prevents the development of myocardial failure in gene-targeted mice. *Proc. Natl. Acad. Sci. U.S.A.* 95, 7000–7005.
- (31) Raake, P. W., Schlegel, P., Ksienzyk, J., Reinkober, J., Barthelmes, J., Schinkel, S., Pleger, S., Mier, W., Haberkorn, U., Koch, W. J., Katus, H. A., Most, P., and Muller, O. J. (2013) AAV6-bARKct cardiac gene therapy ameliorates cardiac function and normalizes the catecholaminergic axis in a clinically relevant large animal heart failure model. *Eur. Heart J.* 34, 1437–1447.
- (32) Lympertopoulos, A., Rengo, G., Funakoshi, H., Eckhart, A. D., and Koch, W. J. (2007) Adrenal GRK2 upregulation mediates sympathetic overdrive in heart failure. *Nat. Med.* 13, 315–323.
- (33) Bastidas, A. C., Deal, M. S., Steichen, J. M., Guo, Y., Wu, J., and Taylor, S. S. (2013) Phosphoryl transfer by protein kinase A is captured in a crystal lattice. *J. Am. Chem. Soc.* 135, 4788–4798.
- (34) Knighton, D. R., Zheng, J. H., Ten Eyck, L. F., Ashford, V. A., Xuong, N. H., Taylor, S. S., and Sowadski, J. M. (1991) Crystal structure of the catalytic subunit of cyclic adenosine monophosphate-dependent protein kinase. *Science* 253, 407–414.
- (35) Knighton, D. R., Zheng, J. H., Ten Eyck, L. F., Xuong, N. H., Taylor, S. S., and Sowadski, J. M. (1991) Structure of a peptide inhibitor bound to the catalytic subunit of cyclic adenosine monophosphate-dependent protein kinase. *Science* 253, 414–420.
- (36) Johnson, L. N. (2009) Protein kinase inhibitors: contributions from structure to clinical compounds. *Q. Rev. Biophys.* 42, 1–40.
- (37) Kannan, N., Haste, N., Taylor, S. S., and Neuwald, A. F. (2007) The hallmark of AGC kinase functional divergence is its C-terminal tail, a *cis*-acting regulatory module. *Proc. Natl. Acad. Sci. U.S.A.* 104, 1272–1277.
- (38) Biondi, R. M., Cheung, P. C., Casamayor, A., Deak, M., Currie, R. A., and Alessi, D. R. (2000) Identification of a pocket in the PDK1 kinase domain that interacts with PIF and the C-terminal residues of PKA. *EMBO J.* 19, 979–988.
- (39) Tamaoki, T., Nomoto, H., Takahashi, I., Kato, Y., Morimoto, M., and Tomita, F. (1986) Staurosporine, a potent inhibitor of phospholipid/Ca<sup>++</sup>-dependent protein kinase. *Biochem. Biophys. Res. Commun.* 135, 397–402.
- (40) Prade, L., Engh, R. A., Girod, A., Kinzel, V., Huber, R., and Bossemeyer, D. (1997) Staurosporine-induced conformational changes of cAMP-dependent protein kinase catalytic subunit explain inhibitory potential. *Structure* 5, 1627–1637.
- (41) Ward, N. E., and O'Brian, C. A. (1992) Kinetic analysis of protein kinase C inhibition by staurosporine: evidence that inhibition entails inhibitor binding at a conserved region of the catalytic domain but not competition with substrates. *Mol. Pharmacol.* 41, 387–392.
- (42) Xu, Z. B., Chaudhary, D., Olland, S., Wolfrom, S., Czerwinski, R., Malakian, K., Lin, L., Stahl, M. L., Joseph-McCarthy, D., Benander, C., Fitz, L., Greco, R., Somers, W. S., and Mosyak, L. (2004) Catalytic domain crystal structure of protein kinase C- $\theta$  (PKC $\theta$ ). *J. Biol. Chem.* 279, 50401–50409.
- (43) Ikuta, M., Kornienko, M., Byrne, N., Reid, J. C., Mizuarai, S., Kotani, H., and Munshi, S. K. (2007) Crystal structures of the N-terminal kinase domain of human RSK1 bound to three different ligands: implications for the design of RSK1 specific inhibitors. *Protein Sci.* 16, 2626–2635.
- (44) Komander, D., Kular, G. S., Bain, J., Elliott, M., Alessi, D. R., and Van Aalten, D. M. (2003) Structural basis for UCN-01 (7-hydroxystaurosporine) specificity and PDK1 (3-phosphoinositide-dependent protein kinase-1) inhibition. *Biochem. J.* 375, 255–262.
- (45) Dong, M., Liao, J. K., Fang, F., Lee, A. P., Yan, B. P., Liu, M., and Yu, C. M. (2012) Increased Rho kinase activity in congestive heart failure. *Eur. J. Heart Failure* 14, 965–973.
- (46) Shi, J., Zhang, Y. W., Yang, Y., Zhang, L., and Wei, L. (2010) ROCK1 plays an essential role in the transition from cardiac hypertrophy to failure in mice. *J. Mol. Cell. Cardiol.* 49, 819–828.
- (47) Zhao, Z., and Rivkees, S. A. (2004) Rho-associated kinases play a role in endocardial cell differentiation and migration. *Dev. Biol.* 275, 183–191.
- (48) Kast, R., Schirok, H., Figueroa-Perez, S., Mittendorf, J., Gnoth, M. J., Apeler, H., Lenz, J., Franz, J. K., Knorr, A., Hutter, J., Lobell, M., Zimmermann, K., Munter, K., Augstein, K. H., Ehmke, H., and Stasch, J. P. (2007) Cardiovascular effects of a novel potent and highly selective azaindole-based inhibitor of Rho-kinase. *Br. J. Pharmacol.* 152, 1070–1080.
- (49) Thal, D. M., Homan, K. T., Chen, J., Wu, E. K., Hinkle, P. M., Huang, Z. M., Chuprun, J. K., Song, J., Gao, E., Cheung, J. Y., Sklar, L. A., Koch, W. J., and Tesmer, J. J. (2012) Paroxetine is a direct inhibitor of G protein-coupled receptor kinase 2 and increases myocardial contractility. *ACS Chem. Biol.* 7, 1830–1839.
- (50) Jacobs, M., Hayakawa, K., Swenson, L., Bellon, S., Fleming, M., Taslimi, P., and Doran, J. (2006) The structure of dimeric ROCK I reveals the mechanism for ligand selectivity. *J. Biol. Chem.* 281, 260–268.
- (51) Breitenlechner, C., Gassel, M., Hidaka, H., Kinzel, V., Huber, R., Engh, R. A., and Bossemeyer, D. (2003) Protein kinase A in complex with Rho-kinase inhibitors Y-27632, Fasudil, and H-1152P: structural basis of selectivity. *Structure* 11, 1595–1607.
- (52) Sehon, C. A., Wang, G. Z., Viet, A. Q., Goodman, K. B., Dowdell, S. E., Elkins, P. A., Semus, S. F., Evans, C., Jolivette, L. J., Kirkpatrick, R. B., Dul, E., Khandekar, S. S., Yi, T., Wright, L. L., Smith, G. K., Behm, D. J., Bentley, R., Doe, C. P., Hu, E., and Lee, D. (2008) Potent, selective and orally bioavailable dihydropyrimidine inhibitors of Rho kinase (ROCK1) as potential therapeutic agents for cardiovascular diseases. *J. Med. Chem.* 51, 6631–6634.
- (53) Li, R., Martin, M. P., Liu, Y., Wang, B., Patel, R. A., Zhu, J. Y., Sun, N., Pireddu, R., Lawrence, N. J., Li, J., Haura, E. B., Sung, S. S., Guida, W. C., Schonbrunn, E., and Sefti, S. M. (2012) Fragment-based and structure-guided discovery and optimization of Rho kinase inhibitors. *J. Med. Chem.* 55, 2474–2478.
- (54) Patel, R. A., Forinash, K. D., Pireddu, R., Sun, Y., Sun, N., Martin, M. P., Schonbrunn, E., Lawrence, N. J., and Sefti, S. M. (2012) RKI-1447 is a potent inhibitor of the Rho-associated ROCK kinases with anti-invasive and antitumor activities in breast cancer. *Cancer Res.* 72, 5025–5034.
- (55) Pireddu, R., Forinash, K. D., Sun, N. N., Martin, M. P., Sung, S. S., Alexander, B., Zhu, J. Y., Guida, W. C., Schonbrunn, E., Sefti, S. M., and Lawrence, N. J. (2012) Pyridylthiazole-based ureas as inhibitors of Rho associated protein kinases (ROCK1 and 2). *MedChemComm* 3, 699–709.
- (56) Bosanac, T., Hickey, E. R., Ginn, J., Kashem, M., Kerr, S., Kugler, S., Li, X., Olague, A., Schlyer, S., and Young, E. R. (2010) Substituted 2H-isoquinolin-1-ones as potent Rho-kinase inhibitors: part 3, aryl substituted pyrrolidines. *Bioorg. Med. Chem. Lett.* 20, 3746–3749.
- (57) Ginn, J. D., Bosanac, T., Chen, R., Cywin, C., Hickey, E., Kashem, M., Kerr, S., Kugler, S., Li, X., Prokopowicz, A., 3rd, Schlyer, S., Smith, J. D., Turner, M. R., Wu, F., and Young, E. R. (2010) Substituted 2H-isoquinolin-1-ones as potent Rho-kinase inhibitors: part 2, optimization for blood pressure reduction in spontaneously hypertensive rats. *Bioorg. Med. Chem. Lett.* 20, 5153–5156.
- (58) Benovic, J. L., Stone, W. C., Caron, M. G., and Lefkowitz, R. J. (1989) Inhibition of the  $\beta$ -adrenergic receptor kinase by polyanions. *J. Biol. Chem.* 264, 6707–6710.
- (59) Lodowski, D. T., Pitcher, J. A., Capel, W. D., Lefkowitz, R. J., and Tesmer, J. J. (2003) Keeping G proteins at bay: a complex between G protein-coupled receptor kinase 2 and Gbg. *Science* 300, 1256–1262.
- (60) Benovic, J. L., Onorato, J., Lohse, M. J., Dohlman, H. G., Staniszewski, C., Caron, M. G., and Lefkowitz, R. J. (1990) Synthetic peptides of the hamster  $\beta$ -adrenoceptor as substrates and inhibitors of the  $\beta$ -adrenoceptor kinase. *Br. J. Clin. Pharmacol.* 30, 3S–12S.

- (61) Winstel, R., Ihlenfeldt, H. G., Jung, G., Krasel, C., and Lohse, M. J. (2005) Peptide inhibitors of G protein-coupled receptor kinases. *Biochem. Pharmacol.* 70, 1001–1008.
- (62) Quitterer, U., Pohl, A., Langer, A., Koller, S., and Abdalla, S. (2011) A cleavable signal peptide enhances cell surface delivery and heterodimerization of Cerulean-tagged angiotensin II AT1 and bradykinin B2 receptor. *Biochem. Biophys. Res. Commun.* 409, 544–549.
- (63) Fu, X., Koller, S., Abd Alla, J., and Quitterer, U. (2013) Inhibition of G-protein-coupled receptor kinase 2 (GRK2) triggers the growth-promoting mitogen-activated protein kinase (MAPK) pathway. *J. Biol. Chem.* 288, 7738–7755.
- (64) Baameur, F., Hammitt, R. A., Friedman, J., McMurray, J. S., and Clark, R. B. (2014) Biochemical and cellular specificity of peptide inhibitors of G protein-coupled receptor kinases. *Int. J. Pept. Res. Ther.* 20, 1–12.
- (65) Baameur, F., Morgan, D. H., Yao, H., Tran, T. M., Hammitt, R. A., Sabui, S., McMurray, J. S., Lichtarge, O., and Clark, R. B. (2010) Role for the regulator of G-protein signaling homology domain of G protein-coupled receptor kinases 5 and 6 in  $\beta$  2-adrenergic receptor and rhodopsin phosphorylation. *Mol. Pharmacol.* 77, 405–415.
- (66) Mayer, G., Wulfflen, B., Huber, C., Brockmann, J., Flicke, B., Neumann, L., Hafnerbradl, D., Klebl, B. M., Lohse, M. J., Krasel, C., and Blind, M. (2008) An RNA molecule that specifically inhibits G-protein-coupled receptor kinase 2 in vitro. *RNA* 14, 524–534.
- (67) Tesmer, V. M., Lennarz, S., Mayer, G., and Tesmer, J. J. (2012) Molecular mechanism for inhibition of G protein-coupled receptor kinase 2 by a selective RNA aptamer. *Structure* 20, 1300–1309.
- (68) Kassack, M. U., Hogger, P., Gschwend, D. A., Kameyama, K., Haga, T., Graul, R. C., and Sadee, W. (2000) Molecular modeling of G-protein coupled receptor kinase 2: docking and biochemical evaluation of inhibitors. *AAPS PharmSci* 2, E2.
- (69) Iino, M., Furugori, T., Mori, T., Moriyama, S., Fukuzawa, A., and Shibano, T. (2002) Rational design and evaluation of new lead compound structures for selective  $\beta$ ARK1 inhibitors. *J. Med. Chem.* 45, 2150–2159.
- (70) Cho, S. Y., Lee, B. H., Jung, H., Yun, C. S., Ha, J. D., Kim, H. R., Chae, C. H., Lee, J. H., Seo, H. W., and Oh, K. S. (2013) Design and synthesis of novel 3-(benzo[d]oxazol-2-yl)-5-(1-(piperidin-4-yl)-1H-pyrazol-4-yl)pyridin-2-amine derivatives as selective G-protein-coupled receptor kinase-2 and -5 inhibitors. *Bioorg. Med. Chem. Lett.* 23, 6711–6716.
- (71) Palczewski, K., Kahn, N., and Hargrave, P. A. (1990) Nucleoside inhibitors of rhodopsin kinase. *Biochemistry* 29, 6276–6282.
- (72) Loomis, C. R., and Bell, R. M. (1988) Sangivamycin, a nucleoside analogue, is a potent inhibitor of protein kinase C. *J. Biol. Chem.* 263, 1682–1692.
- (73) Osada, H., Sonoda, T., Tsunoda, K., and Isono, K. (1989) A new biological role of sangivamycin; inhibition of protein kinases. *J. Antibiot.* 42, 102–106.
- (74) Boguth, C. A., Singh, P., Huang, C. C., and Tesmer, J. J. (2010) Molecular basis for activation of G protein-coupled receptor kinases. *EMBO J.* 29, 3249–3259.
- (75) Kulanthaivel, P., Hallock, Y. F., Boros, C., Hamilton, S. M., Janzen, W. P., Ballas, L. M., Loomis, C. R., Jiang, J. B., Katz, B., Steiner, J. R., and Clardy, J. (1993) Balanol – a novel and potent inhibitor of protein-kinase-C from the fungus *Verticillium balanoides*. *J. Am. Chem. Soc.* 115, 6452–6453.
- (76) Setyawan, J., Koide, K., Diller, T. C., Bunnage, M. E., Taylor, S. S., Nicolaou, K. C., and Brunton, L. L. (1999) Inhibition of protein kinases by balanol: specificity within the serine/threonine protein kinase subfamily. *Mol. Pharmacol.* 56, 370–376.
- (77) Tesmer, J. J., Tesmer, V. M., Lodowski, D. T., Steinhagen, H., and Huber, J. (2010) Structure of human G protein-coupled receptor kinase 2 in complex with the kinase inhibitor balanol. *J. Med. Chem.* 53, 1867–1870.
- (78) Narayana, N., Diller, T. C., Koide, K., Bunnage, M. E., Nicolaou, K. C., Brunton, L. L., Xuong, N. H., Ten Eyck, L. F., and Taylor, S. S. (1999) Crystal structure of the potent natural product inhibitor balanol in complex with the catalytic subunit of cAMP-dependent protein kinase. *Biochemistry* 38, 2367–2376.
- (79) Takeda Pharmaceutical Company Ltd., Ikeda, S., Keneko, M., and Fujiwara, S. (2007) Cardiotonic agent comprising GRK inhibitor. World Patent WO2007034846, March 29.
- (80) Thal, D. M., Yeow, R. Y., Schoenau, C., Huber, J., and Tesmer, J. J. (2011) Molecular mechanism of selectivity among G protein-coupled receptor kinase 2 inhibitors. *Mol. Pharmacol.* 80, 294–303.
- (81) Edwards, B. S., Zhu, J., Chen, J., Carter, M. B., Thal, D. M., Tesmer, J. J., Graves, S. W., and Sklar, L. A. (2012) Cluster cytometry for high-capacity bioanalysis. *Cytometry, Part A* 81, 419–429.
- (82) Homan, K. T., Wu, E., Wilson, M. W., Singh, P., Larsen, S. D., and Tesmer, J. J. (2014) Structural and functional analysis of G protein-coupled receptor kinase inhibition by paroxetine and a rationally designed analog. *Mol. Pharmacol.* 85, 237–248.
- (83) Clarke, M., and Dodson, P. M. (2007) PKC inhibition and diabetic microvascular complications. *Best Pract. Res., Clin. Endocrinol. Metab.* 21, 573–586.
- (84) Akamine, P., Madhusudan, Brunton, L. L., Ou, H. D., Canaves, J. M., Xuong, N. H., and Taylor, S. S. (2004) Balanol analogues probe specificity determinants and the conformational malleability of the cyclic 3',5'-adenosine monophosphate-dependent protein kinase catalytic subunit. *Biochemistry* 43, 85–96.
- (85) Winn, M. D., Ballard, C. C., Cowtan, K. D., Dodson, E. J., Emsley, P., Evans, P. R., Keegan, R. M., Krissinel, E. B., Leslie, A. G., McCoy, A., McNicholas, S. J., Murshudov, G. N., Pannu, N. S., Potterton, E. A., Powell, H. R., Read, R. J., Vagin, A., and Wilson, K. S. (2011) Overview of the CCP4 suite and current developments. *Acta Crystallogr., Sect. D: Biol. Crystallogr.* 67, 235–242.
- (86) Anand, G., Taylor, S. S., and Johnson, D. A. (2007) Cyclic-AMP and pseudosubstrate effects on type-I A-kinase regulatory and catalytic subunit binding kinetics. *Biochemistry* 46, 9283–9291.